Enforcement of stem-cell dormancy by nucleophosmin mutation is a critical determinant of unrestricted self-renewal during myeloid leukemogenesis

Maria Elena Boggio Merlo,[1*] Maria Mallardo,[1*] Lucilla Luzi,[1*] Giulia De Conti,[1] Chiara Caprioli,[1] Roman Hillje,[1] Mario Faretta,[1] Cecilia Restelli,[1] Andrea Polazzi,[1] Valentina Tabanelli,[2] Angelica Calleri,[2] Stefano Pileri,[2,3] Pier Giuseppe Pelicci[1,4] and Emanuela Colombo[1,4]

[1]Department of Experimental Oncology, European Institute of Oncology (IEO), IRCCS, Milan; [2]Unit of Haemato-Pathology, European Institute of Oncology, Milan; [3]Department of Experimental, Diagnostic and Specialty Medicine, Bologna University School of Medicine, Bologna and [4]Department of Oncology and Haemato-Oncology, University of Milan, Milan, Italy

**MEBM, MM and LL contributed equally as first authors.*

Correspondence: E. Colombo
emanuela.colombo@ieo.it

P.G. Pelicci
piergiuseppe.pelicci@ieo.it.

Received: September 9, 2024.
Accepted: March 6, 2025.
Early view: March 13, 2025.

https://doi.org/10.3324/haematol.2024.286577

Abstract

Mutations in the *NPM1* gene (NPMc$^+$) and in the *FLT3* gene (FLT3-ITD) represent the most frequent co-occurring mutations in acute myeloid leukemia (AML), yet the cellular and molecular mechanisms of their co-operation remain largely unexplored. Using mouse models that faithfully recapitulate human AML, we investigated the impact of these oncogenes on pre-leukemic and leukemic hematopoietic stem cells (HSC), both separately and in combination. While both NPMc$^+$ and Flt3-ITD promote the proliferation of pre-leukemia HSC, only NPMc$^+$ drives extended self-renewal by preventing the depletion of the quiescent HSC pool. Quiescent HSC have a dynamic equilibrium between dormant and active states, which respectively support self-renewal and regenerative hematopoiesis. Transcriptional profiling of these dormant and active states revealed that not only does NPMc$^+$ stimulate the transition from dormancy to activity, but it also reinforces the dormant state, thereby ensuring the replenishment of dormant HSC. Intriguingly, the co-expression of NPMc$^+$ and Flt3-ITD engenders a novel phenotypic state within quiescent HSC, whereby dormancy and activity co-exist within a single cell. We posit that this unique state fuels the *in vivo* expansion of self-renewing HSC and facilitates the rapid selection of leukemia-initiating cells. Pharmacological inhibition of the dormancy-related TGFβ1 pathway effectively reduces the self-renewal capacity of leukemia stem cells and extends survival in our mouse models. Collectively, these findings demonstrate that enforcement of HSC dormancy is a critical determinant of unrestricted self-renewal during leukemogenesis and, as such, represents a compelling target for the development of novel anti-leukemic therapies.

Introduction

Acute myeloid leukemia (AML) progression is driven by the accumulation of multiple genetic mutations (typically 2-6 recurrent mutations). These mutations confer different adaptive phenotypes to the affected cells, leading to clonal evolution and to increasing disease severity.[1] Mutations in the nucleophosmin gene (*NPMc$^+$*) are the most frequent genetic alterations in AML (approx. 30%) and frequently co-occur with mutations in *FLT3* (*FLT3*-ITD) and/or *DNMT3A* (*DNMT3A^{mut}*) genes, suggesting co-operation among these mutations. This hypothesis is supported by studies using transgenic mice expressing double or triple mutant combinations.[2-4]

In patients, the prognosis for *NPM1c$^+$/FLT3-ITD* double-mutant AML remains poor, highlighting the urgent need for new therapeutic strategies. However, the individual contributions of *NPMc$^+$* and *FLT3-ITD* to AML development, as well the cellular and molecular mechanisms underlying their co-operation, remain unclear.

Clonal hematopoiesis (CHIP), characterized by somatic mutations in the peripheral blood (PB) of healthy people,[5] has provided insights into AML clonal evolution. In AML with CHIP carrying mutations of both *NPM1* and *DNMT3A*, *NPMc$^+$* is never found in T lymphocytes. However, in approximately 50% of cases, *NPMc$^+$* is present in myelo-lymphoid and/or granulocyte-monocyte progenitors.[6] Consistently, expression

of NPMc$^+$ in mouse myeloid progenitors, alone or with *Dnmt-3A^{mut}*, induces extended self-renewal and hematopoietic stem cell (HSC) reprogramming, establishing an HSC / progenitor pre-leukemic population that eventually evolves into overt leukemia.[7] *NPM1* mutations typically arise in *de novo* AML, often within the dominant leukemic clone alongside other sub-clonal mutations, such as *FLT3-ITD*,[8,9] and persist at relapse in approximately 90% of patients,[10] suggesting that they have a crucial role in establishing the fully transformed leukemia phenotype (AML-founding mutations). Although *NPM1* mutated AML were recognized as a distinct genetic entity in the revised World Health Organization classification, patients with *NPMc$^+$* exhibit heterogeneity in co-mutation patterns, prognosis, and treatment response.[11]

Transcriptional profiling of a large cohort of NPMc$^+$ AML identified two major subtypes: committed or primitive. The committed subtype, associated with better survival, is enriched in *DNMT3A* mutations, while the primitive subtype, linked to worse survival, is enriched in *FLT3-ITD* mutations, stem / progenitor genes and stem / progenitor-like cells. Notably, *NPMc$^+$* has been observed in HSC-enriched CD34$^+$ cells,[12] myeloid, monocytic, erythroid and megakaryocytic cells in the bone marrow (BM) of NPMc$^+$ AML patients,[13] in the peripheral blood (PB) of pre-leukemic individuals,[14] and in the pre-leukemic HSC.[15] These findings suggest that NPMc$^+$ may target different cell compartments (progenitors or HSC) depending on the clonal development trajectories (CHIP or *de novo* AML) or the specific co-occurring mutations (*DNMT3A* or *FLT3-ITD*). Recent studies have explored how various AML-associated mutations influence the biology of hematopoietic cells during the pre-leukemic phase,[16,17] aiming to uncover underlying oncogenic mechanisms that could drive the development of new therapeutic strategies. Here we demonstrate that the role of NPMc$^+$ in sustaining HSC quiescence through the modulation of dormant and active state of quiescent HSC is critical for the extended self-renewal in pre-leukemic HSC. We also describe the functional effects of NPMc$^+$/FLT3-ITD co-operation during AML initiation and growth.

Methods

Mice and treatments

The conditional *NPM1c^{+}*[2] (NPMc$^+$) and conditional Rosa26-*EYGF*[18] (YFP) strains were crossed to obtain NPM1c$^+$/YFP and control YFP mice. YFP and/or NPMc$^+$ expression *in vitro* was achieved treating BM mononuclear cells (BM-MNC) with recombinant TAT-CRE, as previously reported.[2]

NPMc$^+$/YFP and control YFP mice were crossed with *CreERT*[19] (hereafter CRE) to obtain NPMc$^+$/YFP/CRE or YFP/CRE control mice. Mice were intraperitoneally (i.p.) injected with 1 mg 4-OH-tamoxifen (Sigma) daily for seven days to induce NPMc$^+$ and/or YFP expression. YFP$^+$ BM-MNC were FACS-sorted for the self-renewal assay (as described below).

NPMc$^+$ mice were crossed with MxCre mice[20] (hereafter referred to as Mx) and a mouse strain carrying the *Flt3-ITD* knocked-in mutation (*Flt3$^{+/ITD}$* mice;[21] hereafter referred to as Flt3-ITD) to generate Mx, NPMc$^+$/Mx, Flt3-ITD/Mx,and NPMc$^+$/ Flt3-ITD/Mx mice. To induce NPMc$^+$ expression, animals were injected every other day for ten days with poly(I)-poly(C) (250 μg) (GE Healthcare). Mice were analyzed 21 days post pIpC treatment. 150 mg/kg of 5-Fluorouracil (5-FU) was administered i.p. every seven days.

Acute myeloid leukemia-transplanted mice were administered the TGFβR-I inhibitor LY_364947 (Selleckem) at 10 mg/kg every other day. For the proliferation assay, 5-Bromodeoxy-uridine (BrdU, BD Bioscience) was administered i.p. (1 mg/mouse) twice every 6 hours (hr) and mice were analyzed 12 hr after the first injection. The BrdU Label-Retaining Cell assay (LRA) was performed as previously described.[22]

All mice were euthanized by inhalation of high concentrations of CO_2. Eight- to 12-week-old mice were used throughout the study. All animals were inbred and animal procedures were performed in accordance with Italian Legislation (project identification: 825/202-PR and 1129/2015-PR).

Purification of hematopoietic stem cells and flow cytometer analyses

Bone marrow-mononuclear cells were stained for FACS analysis with the following antibodies (purchased from Bioscence): CD11b (PE-CY7) M1/70 clone, Ly-6G (PE-CY7) RB6-8C5 clone, Ter-119 (PE-CY7) Ter-119 clone, CD3e (PE-CY7) 145-2C11 clone, CD45R (PE-Cy7) RA3-6B2 clone, Ly-6A/E (PerCP-CY5.5) D7 clone, cKit (APC-eFluor780) 2B8 clone, FLK (PE) A2F10 clone, CD34 (FITC/biotinilated) RAM34 clone, streptavidin (eFluor450), CD45.1 (PE/FITC/APC) A20 clone, CD45.2 (PE/FITC/APC) 104 clone.

For intracellular immune-staining, BM-MNC were fixed in Cytofix/Cytoperm™ buffer and stained with anti-Ki67 (Alexafluor 647 conjugated, clone 16A8; Biolegend) and dye Hoechst 33342 (Sigma-Aldrich). For BrDU staining, cells were treated with DNAse (150 μg/mL) and then incubated with an anti-BrdU antibody (APC BrdU Flow kit, BD; dilution 1:100 in 1x Perm/Wash buffer).

Transplantation assays

In the competitive setting, 1x10^6 of CD45.2$^+$ cells were mixed with 1x10^6 competitive wild-type CD45.1$^+$ BM-MNC and intravenously (i.v.) injected into lethally irradiated CD45.1$^+$ mice. Percentage of CD45.1$^+$ and CD45.2$^+$ was evaluated in the PB-MNC for up to four months.

In limiting dilution experiments, different amounts of YFP or NPMc$^+$/YFP cells were mixed with 500,000 CD45.1 BM cells and injected i.v. in lethally irradiated recipients. Engrafted mice had ≥0.1% of YFP$^+$ cells in the PB four months post bone marrow transplantation (BMT). The frequency of LT-HSC was calculated with ELDA software (http://bioinf.wehi.edu.au/software/elda).

Immunofluorescence

Bone marrow-mononuclear cells or FACS-sorted LKS cells were fixed and stained with the anti-NPMc$^+$ antibody (rabbit polyclonal made in house) followed by secondary antibody (Alexa488 Fluor® or Alexa647 Fluor®), and counterstained with DAPI. For quantification, images were collected with an Olympus BX61 microscope controlled by image screening Scan^R software. The analysis was carried out by exploiting the A.M.I.CO. computational platform.[23]

Bioinformatic analyses

A detailed description of the bioinformatic analyses is reported in the *Online Supplementary Methods*.

Results

NPMc$^+$ increases hematopoietic stem cell proliferation and self-renewal

To investigate the effects of NPMc$^+$ on HSC, we used transgenic mice carrying a conditional loxP-flanked allele of the NPMc$^+$ human cDNA inserted in the *Hprt* locus.[2] To follow the expression of the NPMc$^+$ transgene *in vivo*, NPMc$^+$ mice were crossed with a syngeneic strain carrying a loxP-flanked Rosa26-EYGF allele[18] (hereafter referred to as NPMc$^+$/YFP and YFP, respectively). BM-MNC isolated from NPMc$^+$/YFP or control YFP mice were treated *in vitro* with the recombinant TAT-CRE protein and FACS-sorted to separate YFP$^+$ and YFP$^-$ subpopulations. Cells expressing NPMc$^+$ were present only in the YFP$^+$ population of NPMc$^+$/YFP mice (Figure 1A, B).

To examine their repopulating capacity, equal numbers (1x10^6) of YFP$^+$ BM-MNC were co-transplanted into congenic (CD45.1$^+$) mice along with CD45.1 BM-MNCs (1:1 ratio). At all time points, mice reconstituted with NPMc$^+$/YFP cells showed significantly higher proportions of donor white blood cell (WBC) count (Figure 1C), demonstrating that NPMc$^+$ confers higher BM repopulating potential.

We then investigated cell composition and cell cycle properties of the BM LSK cell population (Lin$^-$, Sca$^+$, c-Kit$^+$), composed of long-term HSC (LT-HSC; CD34$^-$ and FLK3$^-$), short-term HSC (ST-HSC; CD34$^+$ and FLK3$^-$), and multi-potent progenitors (MPP; CD34$^+$ and FLK3$^+$). Mice were transplanted with NPMc$^+$/YFP$^+$ or YFP$^+$ BM-MNC and, four months after BMT, they were injected with a short-pulse of BrdU prior to BM recovery and FACS analysis. The NPMc$^+$/YFP$^+$ BM cells showed a significant expansion, in terms of both numbers and percentages, of LSK, LT- and ST-HSC (Figure 1D, E, and F, left panel). Instead, MPP number was unchanged and their frequency decreased accordingly (Figure 1F, right panel). Consistently, the *in vivo* BrdU incorporation assay showed a marked increase in proliferating NPMc$^+$/YFP LSK, LT-HSC and ST-HSC and, to a lesser extent, MPP (*Online Supplementary Figure S1A*). No differences were observed in the frequency of apoptotic cells (*Online Supplementary Figure S1B*). To compare our data with previous studies,[24,25] we analyzed our model using the SLAM markers (see *Online Supplementary Figure S1C* for the FACS gating strategy) and found the same numbers and a slightly decreased percentage of LSK/CD150$^+$/CD48$^-$ HSC, as previously reported (*Online Supplementary Figure S1D*, upper panels). However, introducing the CD34 marker, which distinguishes HSC with long-term self-renewal (CD34$^-$ HSC) from early multipotent progenitors (CD34$^+$ MPP1),[22] showed increased numbers and frequency of CD34$^-$ HSC (*Online Supplementary Figure S1D*, lower panels), thus confirming the expansion of LT-HSC induced by NPMc$^+$.

We next sought to investigate *in vivo* self-renewal by measuring numbers of donor-derived LT-HSC collected from recipient mice after transplantation of equal numbers of LT-HSC (see experimental scheme in Figure 2A). Unfortunately, *in vitro* culturing of NPMc$^+$/YFP BM-MNC with cytokines modulates the expression of lineage markers on HSC,[26] thereby precluding FACS sorting of LT-HSC. Therefore, we crossed the NPMc$^+$/YFP mice with the CMV-CreER^T strain[19] to generate NPMc$^+$/YFP/CRE and YFP/CRE (control) animals, enabling rapid *in vivo* induction of NPMc$^+$ and YFP upon 4-OH-tamoxifen administration. YFP$^+$ BM-MNC were purified from NPMc$^+$/YFP/CRE or YFP/CRE mice and injected into lethally irradiated syngeneic mice (BM inputs). Although before transplantation the numbers of donor LT-HSC were comparable in the NPMc$^+$/YFP/CRE and YFP/CRE samples injected (P=0.15) (Figure 2B), animals transplanted with NPMc$^+$/YFP/CRE cells showed a significantly higher number of LT-HSC at four months after transplantation (P=0.0003) (Figure 1B) and, accordingly, a significantly higher self-renewal quotient[27] (P=0.01) (Figure 1C). To investigate whether expanded NPMc$^+$ HSC preserve their repopulating abilities, we performed a limiting dilution transplantation experiment. The NPMc$^+$/YFP/CRE BM-MNC (collected 4 months after BMT) exhibited a significantly higher HSC frequency, evaluated as competitive repopulating units (CRU) by ELDA software analysis,[28] as compared to YFP/CRE BM-MNC (Figure 1D). This functionally confirmed *in vivo* that NPMc$^+$ expression increases HSC self-renewal and that the expanded pool of NPMc$^+$ HSC is fully competent in repopulating mouse BM upon secondary transplantation.

NPMc$^+$-induced increase in proliferation does not reduce the pool of quiescent hematopoietic stem cells

Recruitment of HSC into the cell cycle is associated with a reduction in quiescent HSC and progressive HSC exhaustion. Therefore, we evaluated the effect of NPMc$^+$ on LT-HSC quiescence using combined analysis of DNA content and expression of the Ki67 proliferation-associated antigen (Figure 3A, left panel). We confirmed an increased fraction of cycling NPMc$^+$ LT-HSC in the Ki67$^+$ population (Ki67$^+$/>2N; S/G2/M population) (Figure 3A, middle panel). Importantly, the percentage of quiescent LT-HSC (G0 cells) was maintained at control levels (Figure 3A, middle panel). However, as the total number of LT-HSC is expanded in NPMc$^+$ BM (Figure

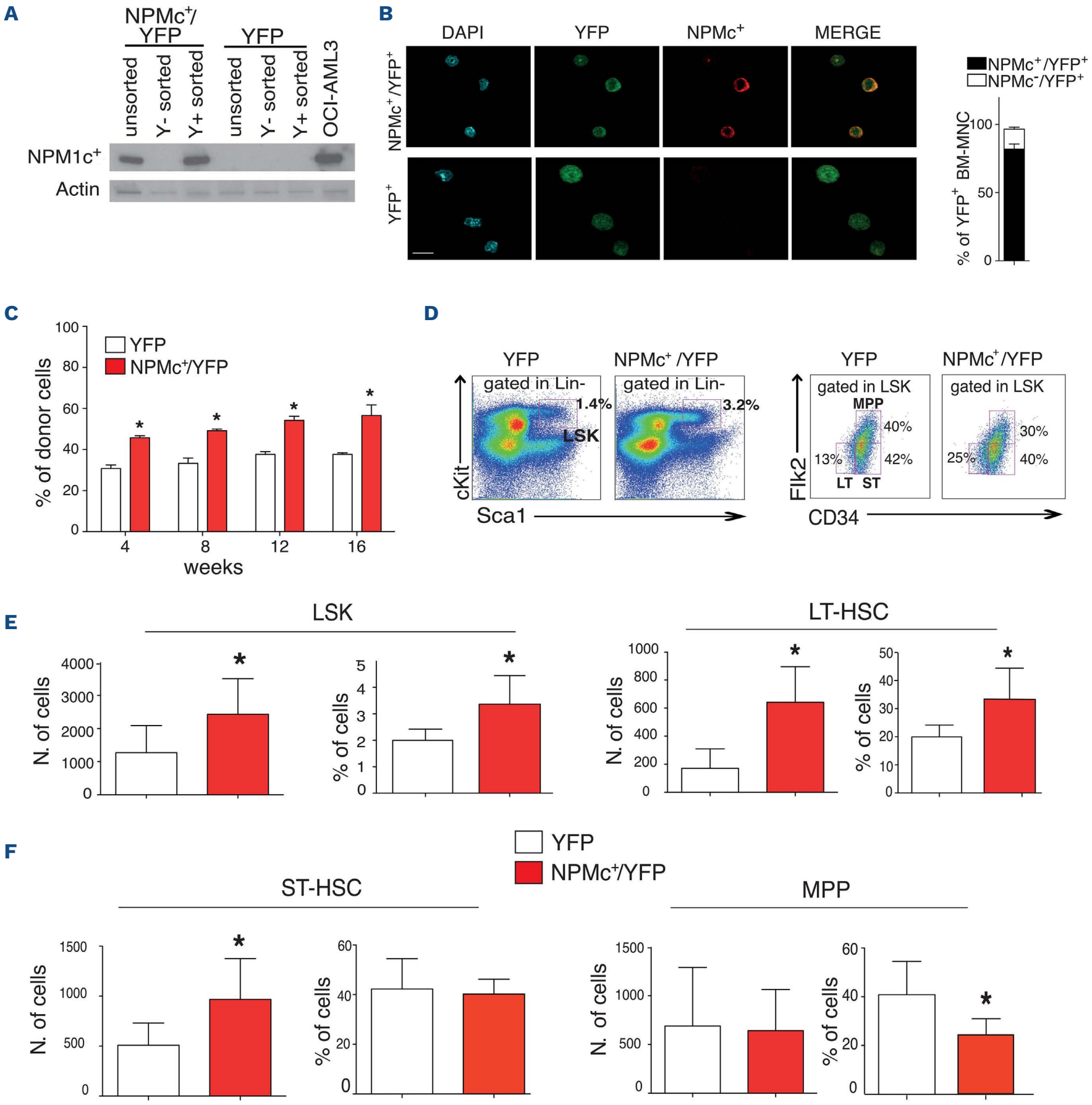

Figure 1. *NPM1c+* expression promotes pre-leukemic hematopoietic stem cell expansion. (A) Western Blot analysis of NPMc$^+$ expression in the YFP$^+$ (Y$^+$) and YFP$^-$ (Y$^-$) fractions after FACS sorting of bone marrow-mononuclear cells (BM-MNC) isolated from NPMc$^+$/YFP and YFP mice and treated *in vitro* with the TAT-CRE. Lysates from the OCI-AML3 NPMc$^+$ cell line were used as positive control. Actin was used as a loading control. (B) (Left) Representative confocal images of anti-NPMc$^+$ immunofluorescence analyses performed on YFP$^+$ cells sorted from NPMc$^+$/YFP and YFP mice. Blue: DAPI; green: YFP; red: NPMc$^+$ (original magnification x256, scale bar 10 μm). (Right) Percentage of NPMc$^+$ cells within the YFP$^+$ sorted population. (C) Competitive bone marrow transplant (BMT, 1:1 ratio): percentage of CD45.2$^+$ donor-derived YFP$^+$ cells in the peripheral blood (PB) of transplanted mice at the indicated time points. N=3-5 mice per cohort, graph representative of one of 3 independent experiments (*P<0.05). (D) Representative FACS gating schemes for the analysis of different hematopoietic populations in the BM of YFP and NPMc$^+$/YFP animals. (Left) Gating of the LSK (c-Kit$^+$, Sca-1$^+$, Lin$^-$) population within lineage negative cells. (Right) Gating of long-term hematopoietic stem cells (LT-HSC) (Lin$^-$, Sca-1$^+$, cKit$^+$, CD34$^-$, FLK$^-$), short-term HSC (ST-HSC) (Lin$^-$, Sca1$^+$, cKit$^+$, CD34$^+$, FLK$^-$), and multi-potent progenitors (MPP) (Lin$^-$, Sca1$^+$, cKit$^+$, CD34$^+$, FLK$^+$) within LKS cells. (E and F) Quantification of the subpopulation depicted in (D): numbers (per million of BM-MNC, left panels) and percentages (right panels) of LSK in the Lin$^-$ population (E, left panel) and LT-HSC (E, right panel). ST-HSC (F, left panel) and MPP (F, right panel) in the LSK population, determined by FACS analyses in NPMc$^+$/YFP and YFP BM-MNC. N=3-5 mice per cohort; graph representative of one of 4 independent experiments (*P<0.05).

1F), the absolute number of G0 HSC was also proportionally expanded in the total BM-MNC count (Figure 3A, right panel). The BrdU-based pulse-chasing Labeling Retaining Assay[22] (LRA) (Figure 3B, top panel) confirmed the expanded number of quiescent, label-retaining BrdU$^+$ LT-HSC in the presence of NPMc$^+$ expression (Figure 3B, bottom panel). Furthermore, mice reconstituted with NPMc$^+$/YFP were significantly more resistant to 5-FU treatment than control YFP mice (Figure 3C), demonstrating that quiescent NPMc$^+$ HSC are functionally competent in supporting hematopoiesis.

Collectively, these data show that NPMc$^+$ expression exerts a dual effect on LT-HSC: it induces proliferation and expansion and, simultaneously, maintains quiescence by preserving self-renewal potential.

In NPMc$^+$/ FLT3-ITD co-expressing hematopoietic stem cells, NPMc$^+$ preserves quiescence and prevents exhaustion

It has been shown that Flt3-ITD expressing LT-HSC hyper-proliferate, are reduced in number and exhibit impaired

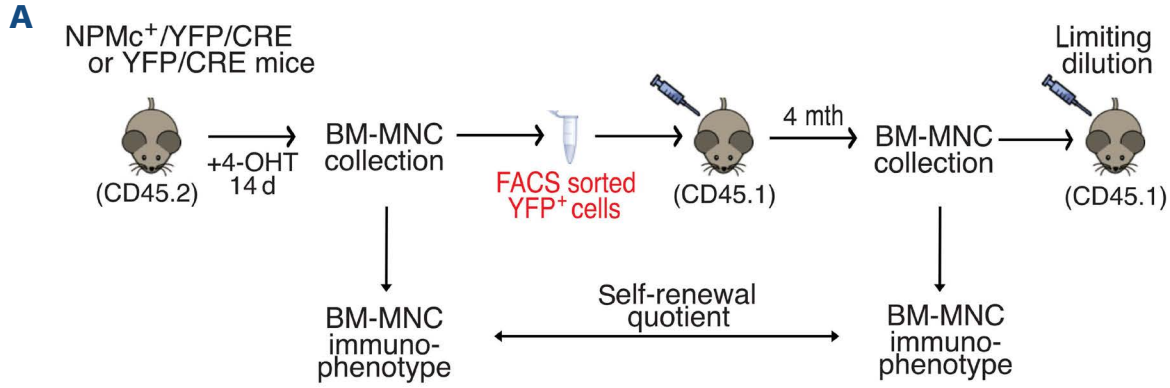

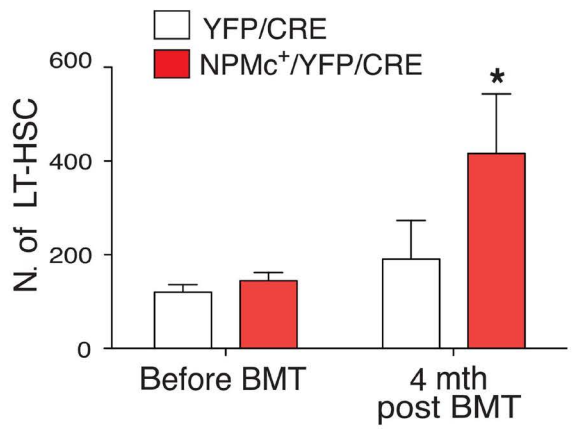

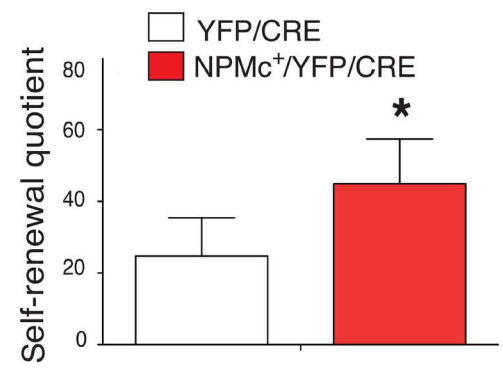

D

	Cell number	N of mice	N of engrafted mice	CRU frequency
WT	500,000	4	4	1:21762
WT	100,000	5	5	
WT	10,000	19	7	
NPMc$^+$	500,000	4	4	1:8676*
NPMc$^+$	100,000	5	5	
NPMc$^+$	10,000	19	13	

*P=0.049

Figure 2. *NPM1c$^+$* expression promotes pre-leukemic hematopoietic stem cell self-renewal. (A) Self-Renewal assay and limiting number bone marrow transplantation (BMT) experimental scheme: YFP/CRE and NPMc$^+$/CRE/YFP recombined bone marrow-mononuclear cells (BM-MNC) have been FACS-analyzed, sorted, and transplanted in recipient mice. After four months (mth), the BM has been collected, FACS-analyzed, and re-transplanted in a limiting dilution assay. (B) Number of long-term hematopoietic stem cells (LT-HSC) in one million BM-MNC derived from 4-OH-tamoxifen (4-OHT)-treated NPMc$^+$/YFP and YFP mice, before (Input) and 4 mth after BMT. N=5 mice per cohort, graph representative of one of 2 independent experiments (*P<0.05). (C) Self-renewal quotient calculated as the ratio between the number of donor LT-HSC in the total BM of recipient mice at 4 mth post BMT, and the numbers of transplanted LT-HSC (*P<0.05). (D) Limiting BMT assay using different amounts of YFP$^+$ FACS-sorted BM-MNC from NPM1c$^+$/YFP or YFP mice (4 mth after the first BMT). Engrafted animals are defined as recipients with >0.1% donor-derived PB cells, 4 mth post BMT. The frequency of functional HSC (Competitive Repopulation Units, CRU) was calculated with the ELDA software. Mean±Standard Deviation values are shown. Unpaired Student *t* test has been applied and significant *P* values are reported. d: days.

self-renewal,[29] suggesting progressive exhaustion of the HSC pool due to constitutive proliferative / differentiative signals delivered by Flt3-ITD. *Flt3*-ITD knock-in mice do not develop AML[29,30] unless they are crossed with animals carrying a co-operative mutation, such as NPMc$^+$. Therefore, we investigated whether co-expression of NPMc$^+$ could rescue the defective Flt3-ITD HSC phenotype. To generate NPMc$^+$/Flt3-ITD compound mice, we first crossed our NPMc$^+$ mice with MxCre mice,[20] and then with a mouse strain carrying the *Flt3-ITD* knock-in mutation (*Flt3*$^{+/ITD}$ mice[21]). The resulting NPMc$^+$/MxCre (hereafter referred to as NPMc$^+$/Mx) and NPMc$^+$/*Flt3*$^{+/ITD}$/MxCre (hereafter referred to as NPMc$^+$/Flt3-ITD/Mx) mice were treated with pIpC to induce NPMc$^+$ expression, while pIpC-treated Mx and Flt3-ITD/Mx animals served as controls.

Ten days after *in vivo* pIpC treatment, NPMc$^+$ was expressed in most PB WBC (*Online Supplementary Figure S2A, B*) and LSK cells of both NPMc$^+$/Mx and NPMc$^+$/Flt3-ITD/Mx mice (*Online Supplementary Figure S2C*). As previously reported, NPMc$^+$/Flt3-ITD/Mx mice developed a fully penetrant AML with a short latency (median, 69 days) (*Online Supplementary Figure S2D*). Numbers of HSC and early progenitors were measured three weeks after pIpC treatment. LT-HSC were increased in the NPMc$^+$/Mx mice, significantly reduced in the Flt3-ITD/Mx, as previously reported,[29] and, strikingly, were rescued by the expression of NPMc$^+$ in the NPMc$^+$/Flt3-ITD/Mx mice (Figure 4A). Moreover, NPMc$^+$/Flt3-ITD/Mx mice showed significant expansion of ST-HSC, MPP and LSK numbers in the BM as compared to Flt3-ITD/Mx animals (Figure 4A). Ki67-negative LT-HSC were expanded in the NPMc$^+$/Mx mice, dramatically reduced in the Flt3-ITD/Mx mice, and re-expanded in the NPMc$^+$/Flt3-ITD/Mx to an extent comparable to control Mx mice (P=0.09) (Figure 4B). Using a 'shortened' LRA protocol (see Figure 4C,

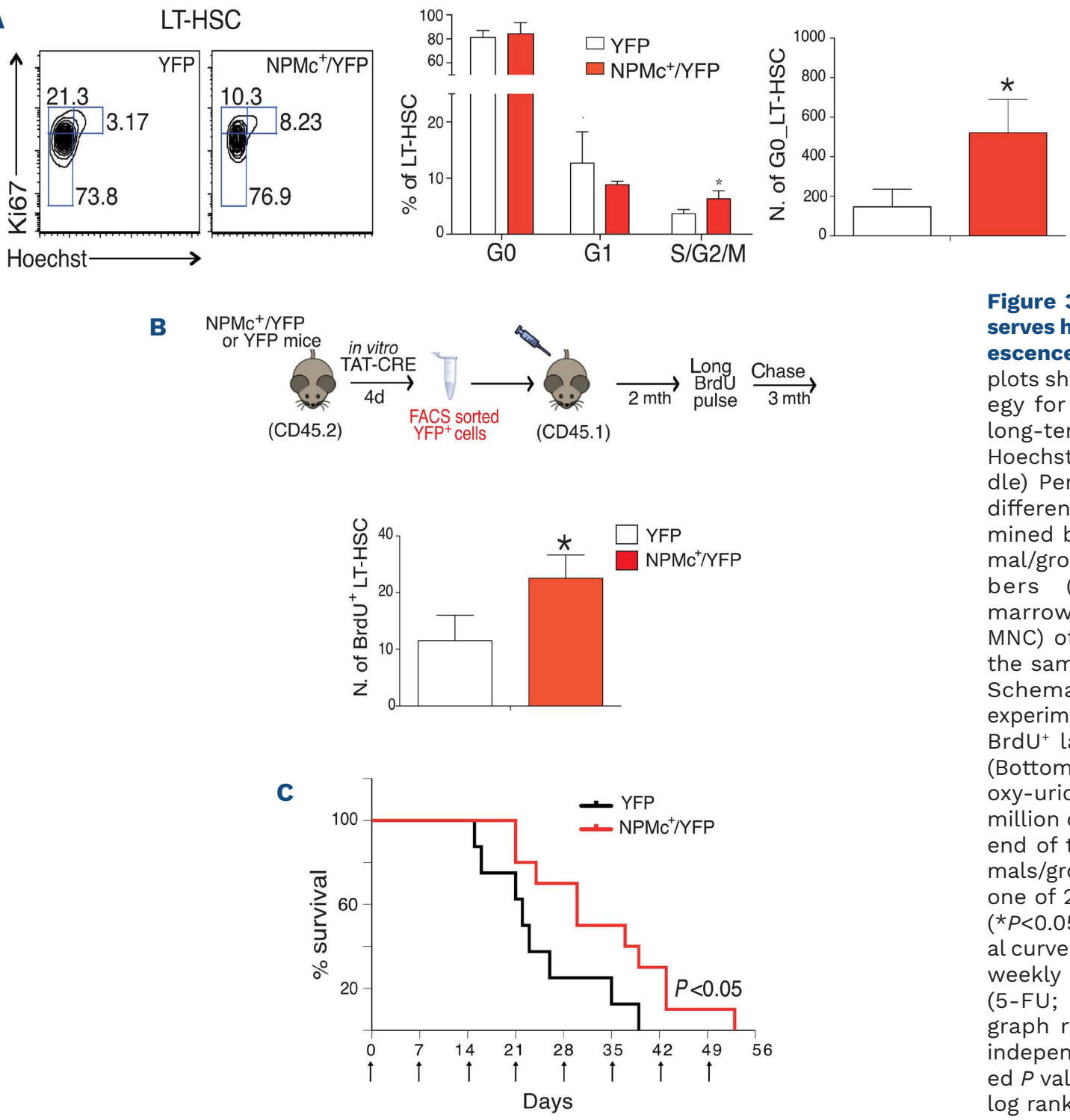

Figure 3. *NPM1c*$^+$ expression preserves hematopoietic stem cell quiescence. (A) (Left) Representative plots showing the FACS gating strategy for the cell cycle analysis of long-term HSC (LT-HSC), based on Hoechst/Ki67 double staining. (Middle) Percentage of LT-HSC in the different cell-cycle phases determined by FACS analyses. N=4 animal/group (*P<0.05). (Right) Numbers (per million of bone marrow-mononuclear cells, BM-MNC) of quiescent (G0) LT-HSC in the same animal cohorts. (B) (Top) Schematic representation of the experimental approach to quantitate BrdU$^+$ label retaining cells (LRC). (Bottom) Numbers of 5-Bromodeoxy-uridine (BrdU)$^+$ LR LT-HSC per million of BM-MNC detected at the end of the chase period. N=4 animals/group, graph representative of one of 2 independent experiments (*P<0.05). (C) Kaplan-Meyer survival curve of YFP and NPMc$^+$/YFP mice weekly treated with 5-fluorouracil (5-FU; N=8 animals per cohort, graph representative of one of 2 independent experiments). Reported P value was calculated with the log rank test. mth: months.

top panel for experimental design), we further observed a significantly decreased number of quiescent/slowly replicating BrdU⁺ LT-HSC in the Flt3-ITD/Mx sample (Figure 4C, bottom left panel), consistent with the reported ability of Flt3-ITD to increase HSC proliferation.[29] Notably, co-expression of NPMc⁺ restored the number of BrdU⁺ LT-HSC to control levels (Figure 4C, bottom left panel). When considering the percentage of BrdU⁺ cells within the LT-HSC compartment, we again observed no variation in NPMc⁺/Mx mice (Figure 4B, top panel) and a significant decrease in Flt3-ITD/Mx mice that was rescued by NPMc⁺ co-expression (Figure 4C, bottom right and middle panels as representative results).

These data demonstrate that NPMc⁺ co-expression preserves quiescence and numbers of Flt3-ITD HSC, thus preventing their functional exhaustion.

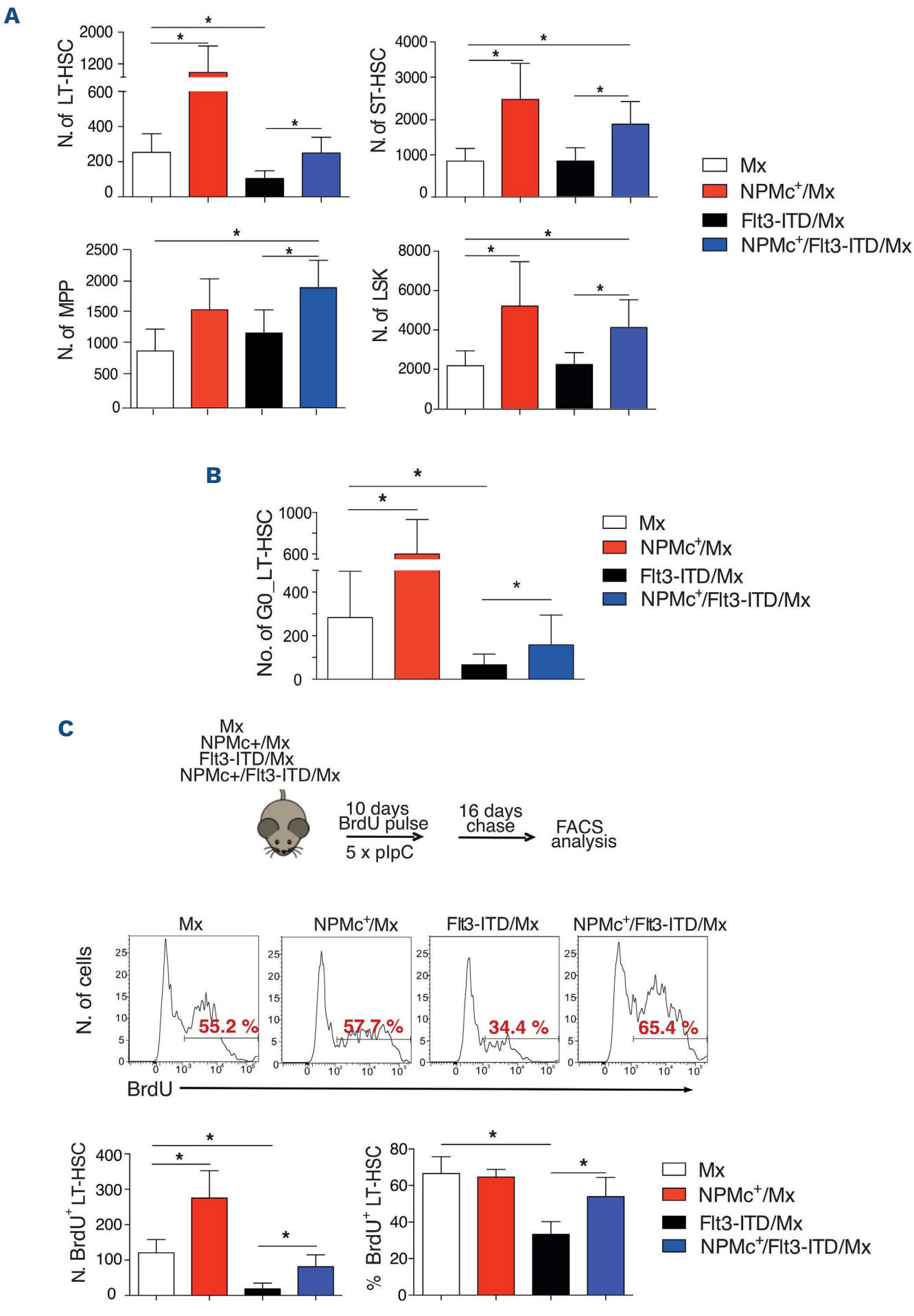

Figure 4. *NPMc⁺* expression restores numbers of total and quiescent long-term hematopoietic stem cells in Flt3-ITD mice. (A) Numbers of hematopoietic stem cells (HSC) / progenitors per million / bone marrow-mononuclear cells (BM-MNC) in Mx, NPMc⁺/Mx, Flt3-ITD/Mx and NPMc⁺/Flt3-ITD/Mx mice. Pool of 3 independent experiments (*P<0.05). (B) Cell cycle analysis by Hoechst/Ki67 staining: numbers per million of BM-MNC of quiescent (G0_2N/Ki67⁻) long-term HSC (LT-HSC). N=12 animal per cohort; pool of 4 independent experiments. (C) (Top) Experimental scheme of the 5-Bromodeoxy-uridine (BrdU) pulse-chasing retaining assay. (Middle) Gating strategy for the analyses of the BrdU retaining LT-HSC after 16 days of chasing. (Bottom) Numbers per million of BM-MNC (left) and percentages within the HSC compartment (right) of BrdU⁺ LT-HSC in NPMc⁺/Mx (N=5), Flt3-ITD/Mx (N=5), NPMc⁺/Flt3-ITD/Mx (N=6), and control Mx-CRE (N=5) mice (*P<0.05).

NPMc⁺ enforces the quiescence transcriptional program in Flt3-ITD hematopoietic stem cells

We then investigated if the biological effects of NPMc⁺ on HSC quiescence correlate with the activation of specific transcriptional programs. Gene expression analyses (by Affymetrix GeneChip) of NPMc⁺/YFP⁺ *versus* YFP⁺ LT-HSC showed upregulation of *HoxA* genes (Figure 5A), which are critical NPMc⁺ targets and a hallmark of NPMc⁺ AML. Gene Set Enrichment Analysis (GSEA) of differentially expressed genes (DEG) (*Online Supplementary Table S1A*) showed enrichment in NPMc⁺ LT-HSC of transcriptional programs specific to HSC (*Online Supplementary Figure S3A, B*), NPMc⁺ or rMLL AML (*Online Supplementary Figure S3C-E*), and LSC (*Online Supplementary Figure S3F*). Most notably, we also found significant enrichment of genes up-regulated in quiescent HSC[31] (Figure 5B) and upregulation of genes involved in HSC self-renewal maintenance through the enforcement of quiescence (e.g., *Mpl*, *Cdkn1a*, *Tgfb1*, *Egr1* and *Angpt1*)[32] (Figure 5C).

Gene Set Enrichment Analysis of DEG in Flt3-ITD/Mx *versus*

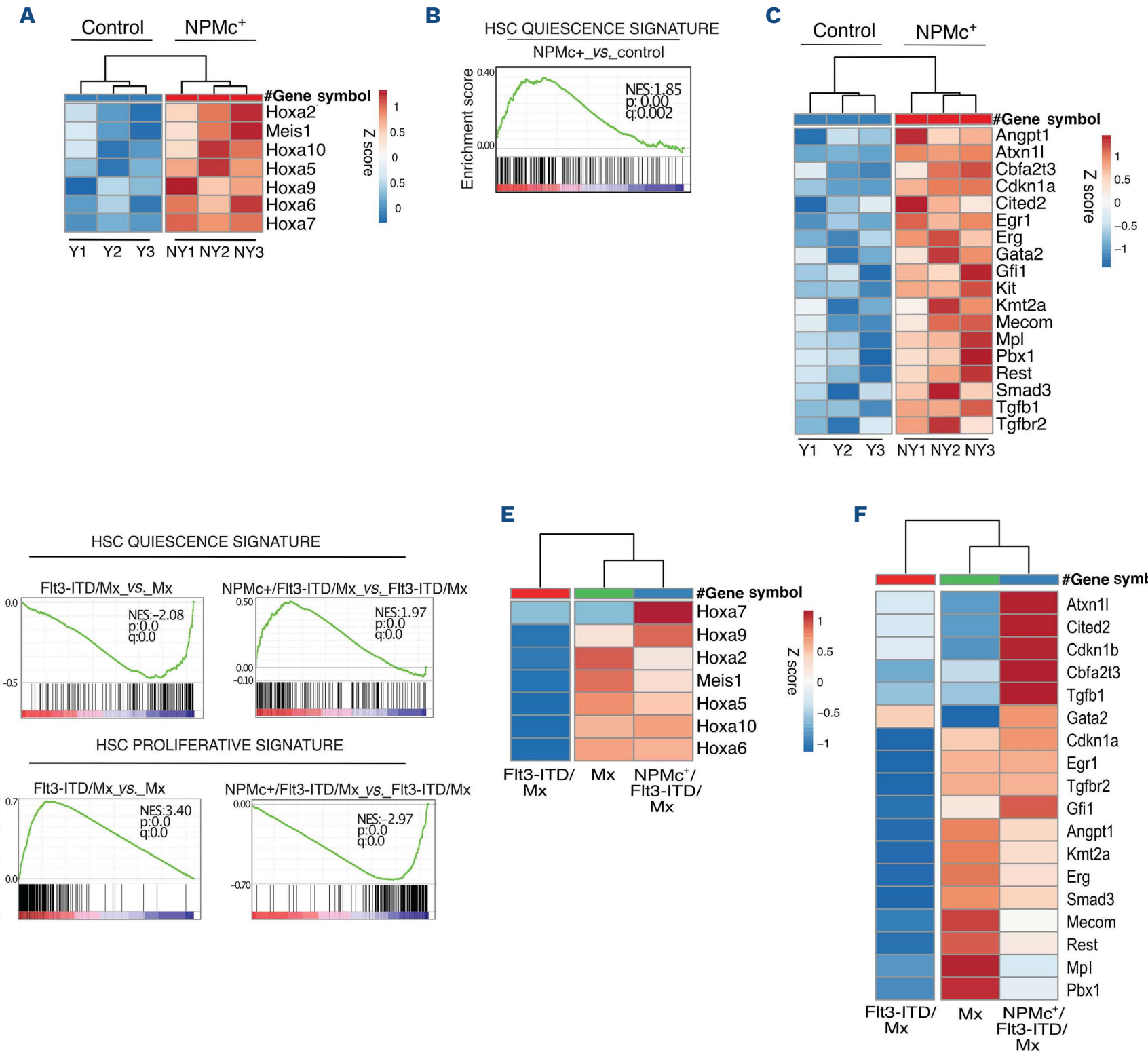

Figure 5. *NPM1c⁺* expression enforces a quiescence transcriptional program. (A and C) Gene-expression analyses of FACS-sorted YFP (Y) and NPMc⁺/YFP (NY) long-term hematopoietic stem cells (LT-HSC). N=4 animals per pool, 3 independent experiments. The heatmaps show the Z-scores of normalized expression values of each triplicate for homeobox genes (A) and genes involved in HSC quiescence maintenance (C); clustering using Euclidean distance and average linkage. (B and D) Gene set enrichment analysis for HSC quiescence- and proliferative-signatures in NPMc⁺ *versus* control (B), Flt3-ITD/Mx *versus* Mx, and NPMc⁺/Flt3-ITD/Mx *versus* Flt3-ITD/Mx (D) LT-HSC. Normalized enrichment score, *P* value (*P*), and false discovery rate (q) are indicated. (E and F) As in (A) and (C), for homeobox genes (E) and quiescence genes (F). Each column represents the average value of 2 independent experiments for Flt3-ITD/Mx; Mx and NPMc⁺/Flt3-ITD/Mx samples.

Mx LT-HSC control animals (*Online Supplementary Table S1B*) showed depletion of quiescence genes and enrichment of proliferation genes in the Flt3-ITD/Mx HSC, both rescued by NPMc$^+$ co-expression (Figure 5D). Similarly, HSC/LSC expression signatures were down-regulated by Flt3-ITD and rescued by NPMc$^+$ (*Online Supplementary Figure S3G, H*). At single gene level, several of the self-renewal / quiescence genes up-regulated by NPMc$^+$ in LT-HSC were markedly down-regulated by Flt3-ITD and rescued by NPMc$^+$ (e.g., *Hoxa5*, *Hoxa10*, *Hoxa6*, *Cdkn1a*, *Egr1*, *Smad3*, *Tgfbr2*), while others, though not affected by Flt3-ITD, were up-regulated in the double mutant LT-HSC (e.g., *Hoxa7*, *Cited2*, *Cdkn1b*, *Tgfb1*) (Figure 5E, F). In conclusion, NPMc$^+$ enforces its transcriptional program in Flt3-ITD/Mx LT-HSC by restoring the expression of critical HSC quiescence genes.

NPMc$^+$ supports both dormant and active states of quiescent hematopoietic stem cells, and the simultaneous expression of dormant and active transcriptional programs in the Flt3-ITD hematopoietic stem cells

Quiescent HSC comprise two phenotypically distinct sub-populations: i) dormant HSC (dHSC), which divide infrequently and possess the highest self-renewal potential; and ii) active HSC (aHSC) which, although quiescent, are poised to divide and support homeostatic hemopoiesis.[22] Notably, HSC can dynamically switch between the two phenotypic states through a series of transient intermediate cell states.[33] We sought to investigate whether NPMc$^+$ and Flt3-ITD alter homeostasis of quiescent HSC, interfering with the equilibrium between active quiescent and active dormant HSC.

Pooled scRNAseq data from our four samples (10,519 cells from Mx, NPMc$^+$/Mx, Flt3-ITD/Mx and NPMc$^+$/Flt3-ITD/Mx; see *Online Supplementary Methods*, *Online Supplementary Table S2* and *Online Supplementary Figure S4A-C* for UMAP representation and numbers) were ordered along a pseudo-temporal trajectory using the MolO dHSC gene signature as reference[33,34] (Figure 6A, left panel). Consistently, plotting normalized mean expression (NME) of the MolO signature in the trajectory (Figure 6A, right panel), as well as another dHSC-specific signature (Do28) (*Online Supplementary Table S3A* and *Online Supplementary Figure S4D*), revealed a gradual decrease from left to right. Conversely, aHSC-specific (Act152), G1-to-S progression or DNA replication signatures showed a progressive increase (*Online Supplementary Table S3A* and *Online Supplementary Figure S4D*).

To compare patterns of dHSC/aHSC distribution, we divided cells along the pseudo-time trajectory in three consecutive groups (Groups 1-3 from left to right; see density plot in *Online Supplementary Figure S4E*), with Group 1 enriched for dHSC, Group 3 enriched for aHSC, and Group 2 comprising cells transitioning between the two states. We identified dormant and active genes differentially expressed among the different groups and samples (*Online Supplementary Table S3B*) and plotted their NME values along the pseudo-time trajectory of each sample (Figure 6B and C for dormant and active genes, respectively). We then established NME cut-off values for dormant and active genes, above which cells were classified as dHSC and aHSC, respectively (Figure 6B-a, C-a). Cells below both cut-off values were considered to be transiting between the two phenotypic states (trHSC). We applied the same thresholds to all four samples (Figure 6B, C, panels b, c, and d) and, for each sample, we calculated the numbers and frequencies of dHSC, aHSC and trHSC (detailed in *Online Supplementary Table S3C*), as well as the mean average expression of dormant and active gene signatures (Figure 6D, E).

NPMc$^+$/Mx LT-HSC exhibited increased numbers of aHSC (35.4% *vs*. 15.1% in control cells) and a shift of the pseudo-time trajectory toward its right end, as evidenced by the expansion of Group 3 aHSC (30% *vs*. 9.3% in control cells) (Figure 6B, C and *Online Supplementary Table S3C)*. This accelerated transition toward aHSC correlates with increased expression of active genes (Figure 6E), yet it was not accompanied by the depletion of Group 1 dHSC (20.2% *vs*. 18.4% in control cells) (*Online Supplementary Table S3C*), and correlated with higher expression of dormant genes (Figure 6D).

The trajectory of Flt3-ITD/Mx HSC was characterized by a marked relocation of dHSC from Group 1 to Group 2 (24.2% *vs.* 11.5% in control cells) in the absence of significant variations in the total number of dHSC (32.4% *vs*. 30.1% in control cells). aHSC were moderately expanded (19.6% *vs*. 15% in control cells) and showed a mild upregulation of active genes (Figure 6E). Thus, Flt3-ITD induces irreversible commitment of dHSC towards a more active state, which may result in reduced self-renewal and progressive exhaustion, as observed *in vivo*.

The NPMc$^+$/Flt3-ITD/Mx pseudo-time trajectory showed pronounced accumulation of HSC in Group 2 (80.1% *vs*. 56% in control cells) (*Online Supplementary Table S3C*), accompanied by a strong depletion of Group 1 dHSC (1.1% *vs*. 18.4% in control cells) and increased numbers of both aHSC (49.4% *vs*. 15.1% in control cells) and dHSC (58.3% *vs*. 30.1% in control cells). Virtually all dHSC (>90%) and most aHSC (approx. 80%) were localized in Group 2, suggesting an overlap of the two phenotypic states at single cell level. Indeed, while in Mx, NPMc$^+$/Mx and Flt3-ITD/Mx samples the dormant and active states were mutually exclusive, NPMc$^+$/Flt3-ITD/Mx HSC showed a high percentage of cells displaying, at single cell level, both dormant and active states (daHSC; 32% *vs*. 0.4% in control cells, mainly located in Group 2) (*Online Supplementary Table S3C*). The HSC with this 'new', intermediate phenotypic state were characterized by increased expression of both dormant and active genes, as compared to control LT-HSC (Figure 6D, E) and, remarkably, higher expression of dormant genes also when compared to dHSC in the same sample (Figure 6D). These data demonstrate that the NPMc$^+$ and Flt3-ITD co-operation results in the integration of their pathogenic signals within a new HSC phenotypic state that can, in principle, proliferate without losing its self-renewal potential.

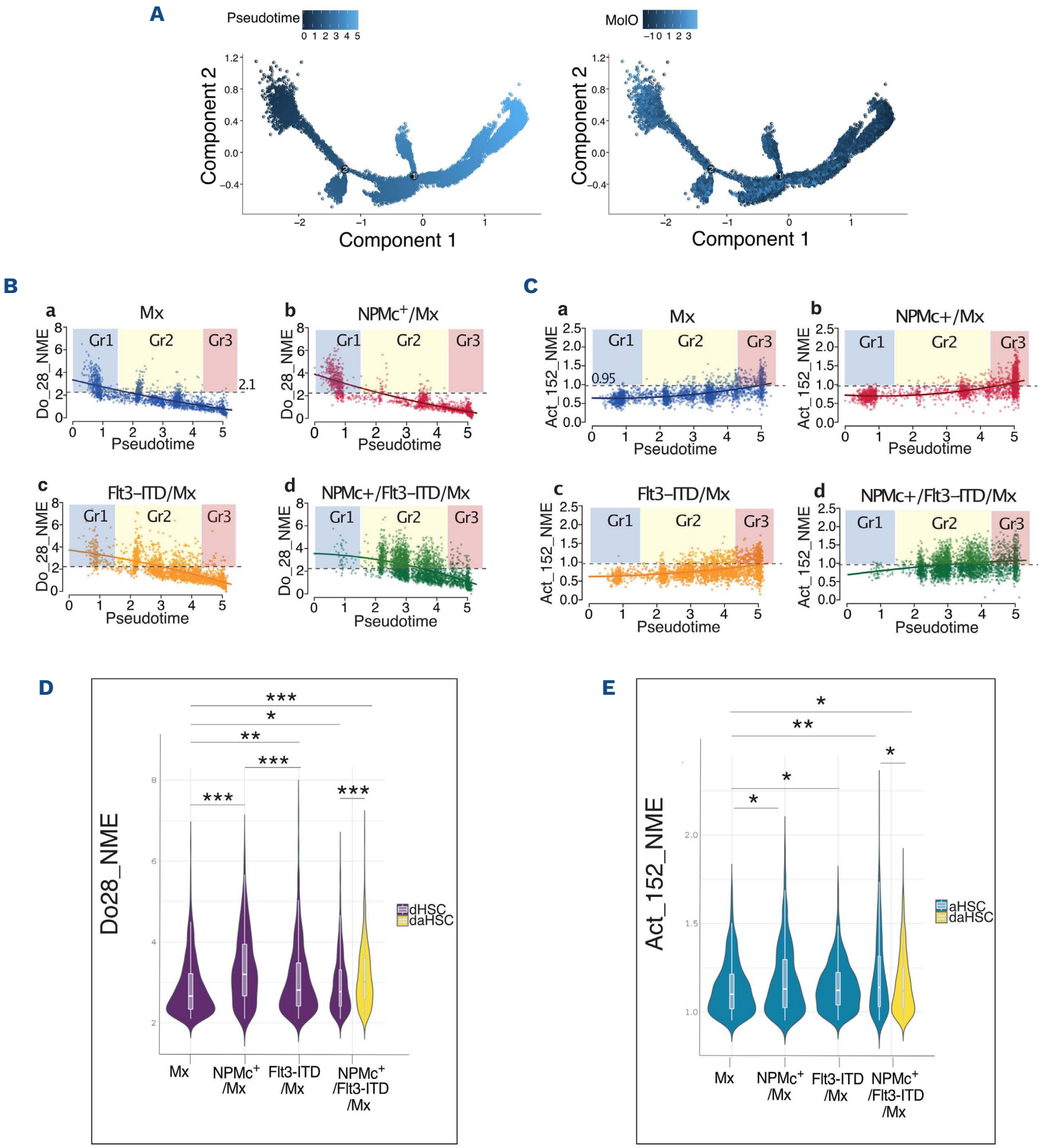

Figure 6. *NPMc⁺* expression promotes hematopoietic stem cell dormancy. (A) (Left) Pseudo-time trajectory of pooled scRNA seq data (Mx, NPMc⁺/Mx, Flt3-ITD/Mx, NPMc⁺/Flt3-ITD/Mx) depicting the transition from the dormant to the active state of long-term hematopoietic stem cells (LT-HSC); pseudo-time progression is represented by the color-code dark (dormant) to light (active) blue. (Right) Color-coded normalized mean expression (NME) of the MoLO gene-signature along the pseudo-time trajectory. High MoLO expression (light blue) defined dormant state while low MoLO expression (dark blue) defined the active state. (B and C) Scatter plots of NME values of dormant (B) and active (C) genes by pseudo-time in the four samples (sig_Do and sig_Act gene-lists; *Online Supplementary Table S2B*). Colored lines are polynomial fit of data and depict the trend of the NME of each signature in each sample. (B-a and C-a) Horizontal dotted line defines the 99th percentile of the NME distribution of Mx cells in Groups 3 and 1, respectively. Cells above the thresholds are dormant HSC (dHSC) (B) or active HSC (aHSC) (C) and are framed by semi-transparent colored squares, based on group definition. (D and E) Combination of violin and overlaid box plots represent the NME distributions of: sig_Do genes (D) or sig_Act genes (E) in the dHSC or aHSC, respectively, of all samples (only for the NPMc⁺/Flt3-ITD/Mx sample dHSC, aHSC and daHSC are depicted separately). Statistical significance was tested with one-tailed Wilcoxon rank sum test (*P<0.05; **P<10^{-4}; ***P<10^{-10}).

In NPMc$^+$/*Flt3-ITD* acute myeloid leukemia, pharmacological inhibition of the dormancy-related TGFβ pathway reduces leukemia stem cell self-renewal

To investigate the functional role of dormancy in self-renewal regulation of leukemia stem cells (LSC), we focused on TGFβ1, a known promoter of cellular dormancy,[35] and an actionable gene up-regulated in WT and Flt3-ITD/Mx LT-HSC by the expression of NPMc$^+$. Consistently, TGFβ signaling is activated in these cells (Figure 7A, B). We examined the effect of TGFβ1 inhibition on self-renewal of LSC by assessing the repopulating potential of murine NPMc$^+$/Flt3-ITD leukemic cells following *in vivo* treatment with the TGFβR-I inhibitor LY364947 (see Figure 7C for experimental design). Engraftment levels at 10-15 days post transplantation were comparable between animals transplanted with inhibitor-treated and untreated blasts. However, from 30 days post transplantation onwards, mice injected with LY364947-treated blasts showed a progressive decline in PB blast counts (Figure 7D), ultimately leading to improved mouse survival (P<0.01) (see Figure 7E and *Online Supplementary Figure S5B* and *C* for an independent NPMc$^+$/Flt3-ITD AML experiment). Importantly, LY364947 treatment also significantly prolonged survival in mice with established NPMc$^+$/Flt3-ITD leukemia (*Online Supplementary Figure S5A*). Analysis of a published scRNAseq dataset of 16 AML patients with defined genotypes,[36] in which the authors have distinguished LSC-enriched (HSC-like) and progenitor-like (prog-like) blast subpopulations,[37] revealed higher TGFβ1 expression in the HSC-like population as compared to the prog-like population across all 16 samples (Figure 7F, left panel). This difference was observed in both NPMc$^+$ (middle panel) and NPM-wild-type (right panel) samples. To explore the clinical relevance of these findings, we assessed the impact of TGFβ1 expression on overall survival (OS) and cumulative incidence of relapse (CIR) in 200 AML patients from The Cancer Genome Atlas (TCGA) cohort. The optimal TGFβ1 expression cutoff for predicting OS was determined by ROC analyses using clinical and RNAseq data from 173 AML samples (*Online Supplementary Figure S5D*). Patients with high *TGFβ1* expression (N=52) showed significantly shorter OS (P<0.0001) and higher CIR (P<0.007) as compared to patients with low *TGFβ1* expression (N=121) (Figure 7G). Crucially, Cox multiple-regression analyses demonstrated that high *TGFβ1* expression is an independent predictor of both OS and CIR, even when accounting for well-established prognostic factors, including age, WBC counts, and risk classes (Hazard Ratio 1.88, 95% CI: 1.27-2.80, P=0.002) (*Online Supplementary Table S4A, B*).

Gene set enrichment analysis of differentially expressed genes between TGFβ1-high *versus* TGFβ1-low AML samples (*Online Supplementary Table S5*) showed enrichment of TGFβ (*Online Supplementary Figure S5E*), NPMc$^+$ leukemia (*Online Supplementary Figure S5F*), and dormancy (MolO and Do28) (*Online Supplementary Figure S5G*) transcriptional programs in the TGFβ1-high group. Conversely, no enrichment was observed for the aHSC gene signature Act166 (*Online Supplementary Figure S5G*). Analysis of high/low *TGFβ1* expression across different cytogenetic and molecular types of AML suggested a trend toward an association between high *TGFβ1* expression and *NPM1* mutations (*Online Supplementary Table S4C*). However, high *TGFβ1* expression was also observed in other molecular types, including AML with complex karyotypes, recurrent translocations, or *FLT3* mutations, indicating that increased TGFβ signaling and enhanced dormancy programs may be a general characteristic of poor prognosis AML.

Discussion

We investigated cell cycle and self-renewal properties of pre-leukemic and LSC expressing NPMc$^+$ and/or *Flt3-ITD*, the most frequent co-occurring mutations in AML patients. Our findings demonstrate that NPMc$^+$ expression exerts both transcriptional and functional effects on the HSC compartment. HSC expressing NPMc$^+$ were increased in numbers, displayed higher BM repopulating potential, and increased *in vivo* self-renewal ability. This strongly supports the notion that NPMc$^+$ confers a pre-leukemic phenotype in HSC, consistent with previous observations in *de novo* AML, where *NPM1* mutations are frequently associated with a stem-like phenotype[11] and can be found in the residual pre-leukemic HSC.[15] Therefore, NPMc$^+$ might be critical for establishing a pre-leukemic state, by imposing aberrant self-renewal in either myeloid progenitors or HSC, depending on the specific AML development trajectory and associated co-mutations. Recognizing the specific contribution of NPMc$^+$ in AML development could have significant implications for patient prognostication and treatment as previously demonstrated, in preclinical and clinical models, for the r-*MLL* AML.[38]

We demonstrated that NPMc$^+$ promotes HSC self-renewal by enforcing a quiescence program. Furthermore, NPMc$^+$ imposes its transcriptional program on Flt3-ITD HSC, restoring the quiescent HSC pool and rescuing the hyper-proliferative phenotype of Flt3-ITD HSC. These findings support a model wherein oncogene-induced chronic hyperproliferation impairs HSC self-renewal unless accompanied by signals that increase quiescence (such as those provided by NPMc$^+$ in our model). This concurrent increase in quiescence allows these mutations to be selected and to express their oncogenic potential. We further investigated the integration and co-operation of oncogenic signals from NPMc$^+$ and Flt3-ITD in HSC by analyzing their respective impacts on the dormant *versus* active states of quiescent HSC. To our knowledge, this is the first study that investigates whether and how gene

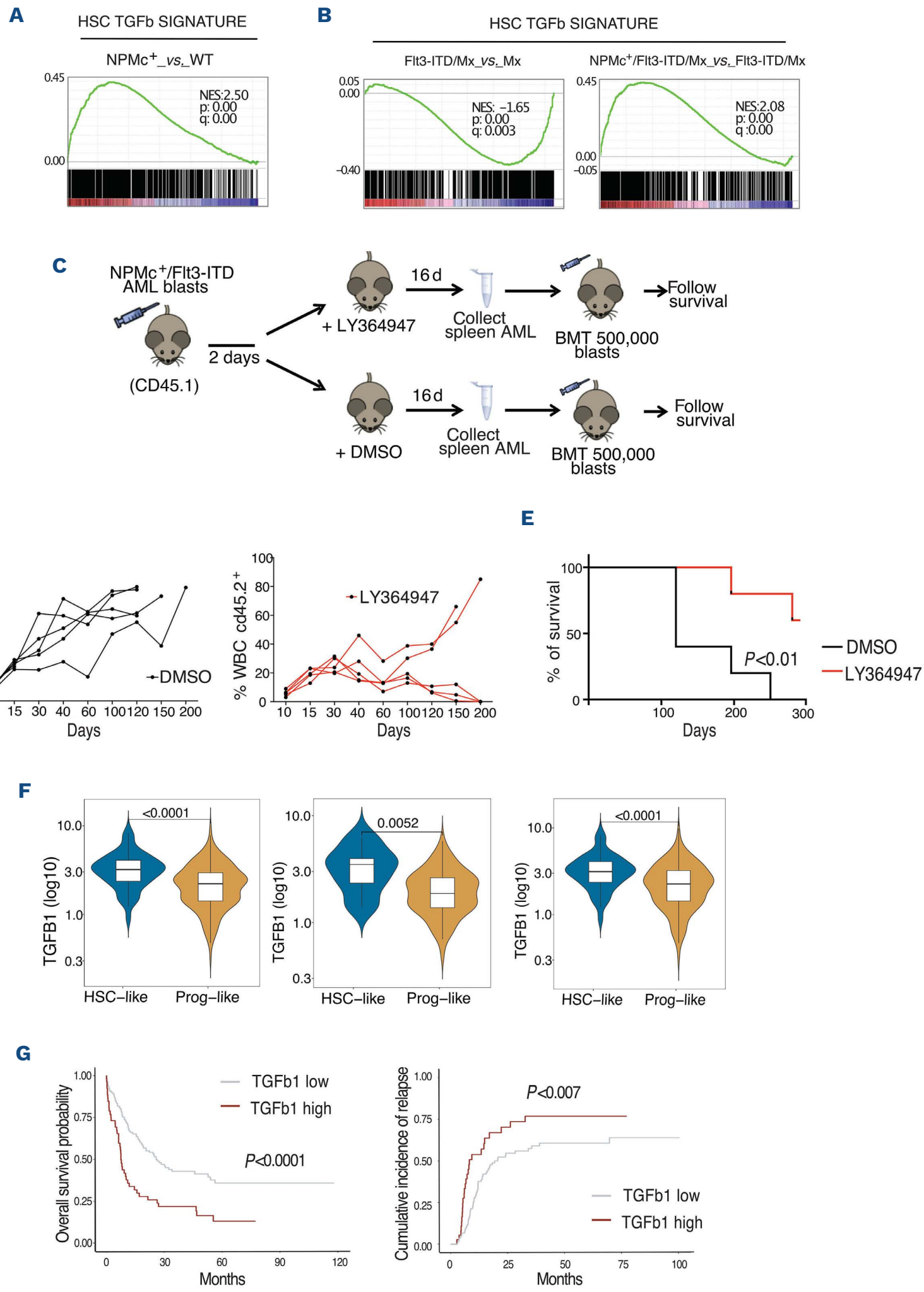

Figure 7. Pharmacological inhibition of the TGFβ pathway affects NPMc⁺/Flt3-ITD leukemic stem cell maintenance. (A and B) Gene set enrichment analysis enrichment plots for the TGFβ signature[41] in NPMc⁺/YFP long-term-hematopoietic stem cells (LT-HSC) *versus* YFP LT-HSC (A) or Flt3-ITD/Mx *versus* Mx LT-HSC and NPMc⁺/Flt3-ITD/Mx *versus* Flt3-ITD/Mx LT-HSC (B). Normalized enrichment score (NES), *P* value by log rank test, and false discovery rate (q) are indicated. (C) Experimental scheme: mice transplanted with a NPMc⁺/Flt3-ITD acute myeloid leukemia (AML) blasts were treated with LY364947 or vehicle every other day for 16 days. At the end of the

Continued on following page.

treatment 500,000 blasts were purified and re-transplanted in secondary recipient mice. (D) Percentage of control or LY364947-treated blasts (CD45.2$^+$) in the peripheral blast (PB) of transplanted (CD45.1$^+$) mice. N=5 animals per group. (E) Kaplan-Meier survival curve of mice transplanted with LY364947-treated or control blasts. N=5 animals per group. (F) Combination of violin and overlaid box plots representing the distributions of *TGFβ1* expression in scRNAseq data set for HSC-like or progenitor-like blasts coming from human AML samples. (Left) All samples (N=16) have been considered regardless of the genotype. (Center) Only the samples carrying the *NPM* mutation have been considered (N=5). (Right) Only samples with NPMwt (N=11) have been considered. Statistical significance was tested with two-sided Wilcoxon test; Confidence Interval 0.95. (G) Overall survival (left) and cumulative incidence of relapse (right) of The Cancer Genome Atlas AML patients based on the expression of *TGFβ1* (normalized RSEM, high≥=0.532, low<0.532). BMT: bone marrow transplant; WBC: white blood cell count.

mutations involved in myeloid malignancies disrupt this equilibrium. We demonstrated that NPMc$^+$ both stimulates the transition from dormant to active HSC states, and promotes the re-entering of active HSC into dormancy by enforcing the dormancy transcriptional program. This dual action replenishes the dHSC pool and prevents self-renewal exhaustion. In contrast, Flt3-ITD induces an irreversible commitment of dHSC toward a more active state. This effect of Flt3-ITD, in co-operation with the enforced dormant and active states induced by NPMc$^+$, creates a new, intermediate phenotypic status where dormant and active states co-exist within individual cells (daHSC). We propose that this novel state allows dormant/active NPMc$^+$/Flt3-ITD HSC to proliferate indefinitely and to accumulate further genetic alterations, facilitating the rapid selection of leukemia-initiating stem cells. This strong NPMc$^+$/Flt3-ITD co-operation at transcriptional level is underpinned by extensive, genome-wide epigenetic rewiring, as reported.[16]

Finally, we demonstrated that pharmacological inhibition of a dormancy-related pathway significantly reduces LSC self-renewal in the context of the fully established leukemic phenotype. Specifically, targeting TGFβ1, a dormancy-related gene up-regulated by NPMc$^+$, significantly reduced the repopulating activity of transplanted NPMc$^+$/Flt3-ITD murine AML and prolonged mouse survival. This suggests that dormancy-related signals are essential for LSC extended self-renewal and leukemia progression, raising the possibility that targeting these pathways could prevent the emergence of drug-resistant cells during primary treatment or the expansion of minimal residual disease after therapy. Notably, we found that high *TGFβ1* expression is an independent predictor of OS and relapse incidence in AML patients across various molecular subtypes, including those without *NPMc$^+$* mutation, suggesting that enforced HSC dormancy may be a common feature of AML with poor prognosis and could be induced by other AML-associated mutations, as previously observed for the AML-associated mutation *NRASG12D*.[39]

In conclusion, our data suggest that increased TGFβ1 expression and enforced dormancy are general characteristics of poor prognosis AML. While our study mainly utilizes preclinical models and the results collected with patient data are preliminary, further investigation, both in preclinical and clinical contexts, is warranted to determine whether *TGFβ1* expression may be a valuable therapeutic marker.[40] Future studies should also explore how TGFβ1 inhibition, in combination with established therapies (e.g., FLT3 inhibitors, alternative chemotherapy regimens, or immune-based therapies) might represent a new therapeutic option for patients with limited response to treatment or those ineligible for induction therapy.

Disclosures

No conflicts of interest to disclose.

Contributions

MEBM, MM, CR and AP conducted the experiments. LL, CC and RH performed the bioinformatic analyses. GDC contributed to in vivo experiments. MF performed the imaging analyses. VT, AC and SP performed the histopathologic analysis. EC and PGP designed the experiments, oversaw the study, and wrote the paper.

Acknowledgments

We thank L. Rotta and the Sequencing Facility at the IEO Genomic Unit. We thank C. Savino for technical assistance and Stefania Averaimo for critical reading of the manuscript. We thank Luca Mazzarella, Fernando Palluzzi and Emanuele Bonetti for bioinformatic advice.

Funding

MEBM and GDC were supported by fellowships from FIRC/AIRC (ref. 19269 and 16342, respectively). This study was supported by the European Research Council advanced grant n. 341131 and AIRC grant (AIRC-IG-2017-20162; to PGP) PRIN 2017, Ricerca Finalizzata 2011 (RF-2011-02347253; to EC). This work was partially supported by the Italian Ministry of Health with funds from Ricerca Corrente and 5x1000.

Data-sharing statement

Affimetrix data are available at: https://www.ncbi.nlm.nih.gov/geo/query/acc.cgi?token=shkveioipryfzyh&acc=GSE94650

RNAseq data and scRNAseq data are available at: https://www.ncbi.nlm.nih.gov/geo/query/acc.cgi?acc=GSE133081

References

1. Welch JS, Ley TJ, Link DC, et al. The origin and evolution of mutations in acute myeloid leukemia. Cell. 2012;150(2):264-278.
2. Mallardo M, Caronno A, Pruneri G, et al. NPMc+ and FLT3_ITD mutations cooperate in inducing acute leukaemia in a novel mouse model. Leukemia. 2013;27(11):2248-2251.
3. Mupo A, Celani L, Dovey O, et al. A powerful molecular synergy between mutant nucleophosmin and Flt3-ITD drives acute myeloid leukemia in mice. Leukemia. 2013;27(9):1917-1920.
4. Vassiliou GS, Cooper JL, Rad R, et al. Mutant nucleophosmin and cooperating pathways drive leukemia initiation and progression in mice. Nat Genet. 2011;43(5):470-475.
5. Bowman RL, Busque L, Levine RL. Clonal hematopoiesis and evolution to hematopoietic malignancies. Cell Stem Cell. 2018;22(2):157-170.
6. Shlush LI, Zandi S, Mitchell A, et al. Identification of pre-leukaemic haematopoietic stem cells in acute leukaemia. Nature. 2014;506(7488):328-333.
7. Uckelmann HJ, Kim SM, Wong EM, et al. Therapeutic targeting of preleukemia cells in a mouse model of NPM1 mutant acute myeloid leukemia. Science. 2020;367(6477):586-590.
8. Papaemmanuil E, Gerstung M, Bullinger L, et al. Genomic classification and prognosis in acute myeloid leukemia. N Engl J Med. 2016;374(23):2209-2221.
9. Miles LA, Bowman RL, Merlinsky TR, et al. Single-cell mutation analysis of clonal evolution in myeloid malignancies. Nature. 2020;587(7834):477-482.
10. Kronke J, Bullinger L, Teleanu V, et al. Clonal evolution in relapsed NPM1-mutated acute myeloid leukemia. Blood. 2013;122(1):100-108.
11. Mer AS, Heath EM, Madani Tonekaboni SA, et al. Biological and therapeutic implications of a unique subtype of NPM1 mutated AML. Nat Commun. 2021;12(1):1054.
12. Martelli MP, Pettirossi V, Thiede C, et al. CD34+ cells from AML with mutated NPM1 harbor cytoplasmic mutated nucleophosmin and generate leukemia in immunocompromised mice. Blood. 2010;116(19):3907-3922.
13. Pasqualucci L, Liso A, Martelli MP, et al. Mutated nucleophosmin detects clonal multilineage involvement in acute myeloid leukemia: impact on WHO classification. Blood. 2006;108(13):4146-4155.
14. Quiros PM, Gu M, Barcena C, Iyer V, Vassiliou GS. NPM1 gene mutations can be confidently identified in blood DNA months before de novo AML onset. Blood Adv. 2022;6(7):2409-2413.
15. Jan M, Snyder TM, Corces-Zimmerman MR, et al. Clonal evolution of preleukemic hematopoietic stem cells precedes human acute myeloid leukemia. Sci Transl Med. 2012;4(149):149ra18.
16. Yun H, Narayan N, Vohra S, et al. Mutational synergy during leukemia induction remodels chromatin accessibility, histone modifications and three-dimensional DNA topology to alter gene expression. Nat Genet. 2021;53(10):1443-1455.
17. Isobe T, Kucinski I, Barile M, et al. Preleukemic single-cell landscapes reveal mutation-specific mechanisms and gene programs predictive of AML patient outcomes. Cell Genom. 2023;3(12):100426.
18. Srinivas S, Watanabe T, Lin CS, et al. Cre reporter strains produced by targeted insertion of EYFP and ECFP into the ROSA26 locus. BMC Dev Biol. 2001;1:4.
19. Feil R, Brocard J, Mascrez B, LeMeur M, Metzger D, Chambon P. Ligand-activated site-specific recombination in mice. Proc Natl Acad Sci U S A. 1996;93(20):10887-10890.
20. Kuhn R, Schwenk F, Aguet M, Rajewsky K. Inducible gene targeting in mice. Science. 1995;269(5229):1427-1429.
21. Lee BH, Tothova Z, Levine RL, et al. FLT3 mutations confer enhanced proliferation and survival properties to multipotent progenitors in a murine model of chronic myelomonocytic leukemia. Cancer Cell. 2007;12(4):367-380.
22. Wilson A, Laurenti E, Oser G, et al. Hematopoietic stem cells reversibly switch from dormancy to self-renewal during homeostasis and repair. Cell. 2008;135(6):1118-1129.
23. Furia L, Pelicci PG, Faretta M. A computational platform for robotized fluorescence microscopy (II): DNA damage, replication, checkpoint activation, and cell cycle progression by high-content high-resolution multiparameter image-cytometry. Cytometry A. 2013;83(4):344-355.
24. Dovey OM, Cooper JL, Mupo A, et al. Molecular synergy underlies the co-occurrence patterns and phenotype of NPM1-mutant acute myeloid leukemia. Blood. 2017;130(17):1911-1922.
25. Loberg MA, Bell RK, Goodwin LO, et al. Sequentially inducible mouse models reveal that Npm1 mutation causes malignant transformation of Dnmt3a-mutant clonal hematopoiesis. Leukemia. 2019;33(7):1635-1649.
26. Chen CL, Faltusova K, Molik M, Savvulidi F, Chang KT, Necas E. Low c-Kit expression level induced by stem cell factor does not compromise transplantation of hematopoietic stem cells. Biol Blood Marrow Transplant. 2016;22(7):1167-1172.
27. Challen GA, Sun D, Jeong M, et al. Dnmt3a is essential for hematopoietic stem cell differentiation. Nat Genet. 2011;44(1):23-31.
28. Hu Y, Smyth GK. ELDA: extreme limiting dilution analysis for comparing depleted and enriched populations in stem cell and other assays. J Immunol Methods. 2009;347(1-2):70-78.
29. Chu SH, Heiser D, Li L, et al. FLT3-ITD knockin impairs hematopoietic stem cell quiescence/homeostasis, leading to myeloproliferative neoplasm. Cell Stem Cell. 2012;11(3):346-358.
30. Li L, Piloto O, Nguyen HB, et al. Knock-in of an internal tandem duplication mutation into murine FLT3 confers myeloproliferative disease in a mouse model. Blood. 2008;111(7):3849-3858.
31. Venezia TA, Merchant AA, Ramos CA, et al. Molecular signatures of proliferation and quiescence in hematopoietic stem cells. PLoS Biol. 2004;2(10):e301.
32. Yamada T, Park CS, Lacorazza HD. Genetic control of quiescence in hematopoietic stem cells. Cell Cycle. 2013;12(15):2376-2383.
33. Cabezas-Wallscheid N, Buettner F, Sommerkamp P, et al. Vitamin A-retinoic acid signaling regulates hematopoietic stem cell dormancy. Cell. 2017;169(5):807-823.e19.
34. Wilson NK, Kent DG, Buettner F, et al. Combined single-cell functional and gene expression analysis resolves heterogeneity within stem cell populations. Cell Stem Cell. 2015;16(6):712-724.
35. Prunier C, Baker D, Ten Dijke P, Ritsma L. TGF-beta family signaling pathways in cellular dormancy. Trends Cancer. 2019;5(1):66-78.
36. van Galen P, Hovestadt V, Wadsworth Ii MH, et al. Single-cell RNA-Seq reveals AML hierarchies relevant to disease progression and immunity. Cell. 2019;176(6):1265-1281.e24.
37. Zeng AGX, Bansal S, Jin L, et al. A cellular hierarchy framework for understanding heterogeneity and predicting drug response in acute myeloid leukemia. Nat Med. 2022;28(6):1212-1223.
38. Krivtsov AV, Figueroa ME, Sinha AU, et al. Cell of origin

determines clinically relevant subtypes of MLL-rearranged AML. Leukemia. 2013;27(4):852-860.
39. Li Q, Bohin N, Wen T, et al. Oncogenic Nras has bimodal effects on stem cells that sustainably increase competitiveness. Nature. 2013;504(7478):143-147.
40. Prajapati SK, Kumari N, Bhowmik D, Gupta R. Recent advancements in biomarkers, therapeutics, and associated challenges in acute myeloid leukemia. Ann Hematol. 2024;103(11):4375-4400.
41. Billing M, Rorby E, May G, et al. A network including TGFbeta/Smad4, Gata2, and p57 regulates proliferation of mouse hematopoietic progenitor cells. Exp Hematol. 2016;44(5):399-409.e5.